Journal of Translational Autoimmunity 12 (2026) 100349

Contents lists available at ScienceDirect

Journal of Translational Autoimmunity

journal homepage: www.sciencedirect.com/journal/journal-of-translational-autoimmunity

Liraglutide prevents lupus-associated diffuse alveolar hemorrhage via inhibiting lymphocyte infiltration and promoting macrophage M2 polarization

Li Jiang [a,b,1], Liting He [a,1], Duo Li [c], Xin Luo [a], Ming Yang [a], Haijing Wu [a], Hai Long [a,*]

[a] Department of Dermatology, Hunan Key Laboratory of Medical Epigenomics, Hunan Provincial Clinical Medicine Research Center for Major Skin Diseases and Skin Health, The Second Xiangya Hospital, Central South University, 139 Middle Renmin Road, Changsha, Hunan 410011, China
[b] Department of Dermatology, Chengdu Second People's Hospital, 10 Qingyun South Street, Chengdu, Sichuan, 610000, China
[c] Department of Pathology, The Second Xiangya Hospital, Central South University, 139 Middle Renmin Road, Changsha, Hunan, 410011, China

ARTICLE INFO

Keywords:
Systemic lupus erythematosus (SLE)
Diffuse alveolar hemorrhage (DAH)
Liraglutide
Macrophage
Polarization

ABSTRACT

Objectives: This study aimed to explore the prophylactic and therapeutic role of liraglutide for lupus-associated diffuse alveolar hemorrhage (DAH).
Methods: A lupus-associated DAH model was established in 6-8-week-old female C57BL/6 mice via intraperitoneal injection of 0.5 mL pristane. Mice were randomized to receive daily intraperitoneal injections of either saline or liraglutide (2 mg/kg/day), starting either 14 days before or on the day of pristane injection, and continuing until 14 days post-injection. Body weight and blood glucose were monitored. Serum levels of anti-dsDNA, ANA, total IgM and IgG were quantified using ELISA. Lung tissues were collected for histopathological analysis with H&E and Prussian blue staining, respectively, characterization of different types of immune cells infiltration with flow cytometry (t-SNE for subset dimensionality reduction) and immunofluorescence, and quantification of protein levels with Western blot.
Results: Liraglutide significantly alleviated pulmonary hemorrhage, as evidenced by reduced lung wet weight, incidence of lung hemorrhage, pulmonary hemosiderin-laden macrophages, and total serum IgG, without affecting body weight or glucose. Mechanistically, liraglutide treatment reduced pulmonary infiltration of multiple T and B lymphocyte subsets (e.g., $CD4^+$, $CD8^+$, $B220^+$), while concurrently increasing alveolar macrophages and promoting M2 macrophage polarization. The phenotypic shift was demonstrated by increased M2 cell numbers, elevated CD206 expression, and downregulation of M1 marker CD86 and upregulation of M2 marker CD163 as confirmed at the protein level.
Conclusion: Liraglutide treatment effectively ameliorates lupus-associated DAH, potentially through modulation of T cells, B cells, and macrophages polarization, offering a novel prophylactic and therapeutic strategy for this fatal complication of lupus.

1. Introduction

Systemic lupus erythematosus (SLE) is a chronic autoimmune disease characterized by the production of autoantibodies and the deposition of immune complexes, which can lead to multi-organ damage [1]. Although the clinical presentation of SLE is highly heterogeneous, pulmonary involvement constitutes a major contributor to morbidity and mortality [2,3]. Among the various pulmonary manifestations, diffuse alveolar hemorrhage (DAH) stands out as one of the most devastating and life-threatening complications [4]. Despite its relatively low incidence, DAH is associated with a strikingly high mortality rate, historically reported to as high as 90 %, even with aggressive interventions [5,6]. The pathogenesis of DAH in SLE is complex and not fully elucidated. Thus, current management primarily relies on broad-spectrum

* Corresponding author. Department of Dermatology, The Second Xiangya Hospital of Central South University, 139 Middle Renmin Road, Changsha, Hunan, 410011, China.
E-mail addresses: jiangli815zeal@163.com (L. Jiang), heliting@csu.edu.cn (L. He), liduo79@csu.edu.cn (D. Li), 248201037@csu.edu.cn (X. Luo), yangming_0216@csu.edu.cn (M. Yang), chriswu1010@csu.edu.cn (H. Wu), dr.hailong@csu.edu.cn (H. Long).
[1] Li Jiang and Liting He contributed equally to this work.

https://doi.org/10.1016/j.jtauto.2026.100349
Received 15 December 2025; Received in revised form 6 January 2026; Accepted 10 January 2026
Available online 12 January 2026

immunosuppression, including high-dose corticosteroids and cyclophosphamide. However, these regimens are often partially effective and associated with significant adverse effects [7]. Consequently, exploring novel therapeutic or prophylactic strategies is urgently needed to improve outcomes for lupus-associated DAH.

The pathogenesis of DAH, though not fully elucidated, is initiated by the deposition of immune complexes (ICs) in alveolar capillaries. This event triggers two distinct yet convergent pathways: a prominent neutrophilic-inflammatory cascade and a macrophage-dominated process [8]. In the inflammatory pathway, IC deposition activates complement and recruit neutrophils, which release neutrophil extracellular traps (NETs), reactive oxygen species, and proteases, directly damaging the endothelium and leading to capillaritis and severe hemorrhage [9]. This innate response can further be orchestrated and amplified by adaptive immunity, in which B cells furnish autoantibodies for IC formation, and T cells perpetuate a pro-inflammatory cytokine milieu [10]. Concurrently, the homeostatic function of alveolar macrophages is disrupted, often skewing toward a pro-inflammatory phenotype that exacerbates tissue injury and correlates positively with hemorrhage severity. Nevertheless, macrophages also play a crucial role in clearing apoptotic bodies, highlighting their dual functions in DAH [11]. Collectively, this intricate network of innate and adaptive immune effectors underscores the limitation of conventional immunosuppressive approaches and emphasizes the importance for novel agents capable of modulating this multifaceted immune dysregulation.

Glucagon-like peptide-1 (GLP-1) receptor agonists (GLP-1RAs), widely used in type 2 diabetes and obesity [12,13], have emerged as promising candidates due to their extra-pancreatic anti-inflammatory and immunomodulatory properties [14]. Existing studies have shown that GLP-1R is not only expressed in pancreatic islets but also on various immune and structural cells in the lung [15,16]. Furthermore, the use of GLP-1RAs has been associated with a reduced risk of developing a spectrum of respiratory diseases, including pneumonia, bronchitis, pulmonary fibrosis, asthma, and chronic obstructive pulmonary disease [17]. Liraglutide, a long-acting GLP-1 analog with a well-established safety profile, exerts potent anti-inflammatory and vascular protective effects beyond glycemic control. Specifically, it has been shown to inhibit the activation of the NLRP3 inflammasome [18,19], reduce the production of pro-inflammatory cytokines (e.g., TNF-α, IL-1β, IL-6) [20,21], and modulate neutrophil activity [22]. Crucially, in models of atherosclerosis and other vascular diseases, liraglutide demonstrates a direct capacity to improve endothelial function and barrier integrity [23–25]. Moreover, treatment with liraglutide markedly reduces lipopolysaccharide (LPS)- or sepsis-induced acute lung injury (ALI) [26–28], attenuates pulmonary inflammation and fibrosis in mice exposed to silica [29], alleviates ischemia/reperfusion injury in lung transplantation [30], and improves lung function in obstructive lung disease [31]. Given these pleiotropic effects as well as the clinical and histopathological similarities between ALI and DAH, we hypothesized that liraglutide might also confer protection in SLE-associated DAH. However, the potential of liraglutide to ameliorate DAH has not yet been investigated.

Therefore, this study was designed to systematically evaluate the efficacy of liraglutide in preventing DAH in a pristane-induced murine lupus model. We comprehensively assess the impact of liraglutide treatment on hemorrhage severity, lung inflammation, and immune cell infiltration of pristane-induced DAH.

2. Materials and methods

2.1. Mice

The C57BL/6 mice purchased from Slack Company (Shanghai, China) were housed under specific pathogen-free (SPF) conditions at the Experimental Animal Center of the Second Xiangya Hospital with ad libitum access to food and water.

To establish a lupus-associated DAH model, female C57BL/6 mice aged 6–8 weeks received a single intraperitoneal (i.p.) injection of 0.5 mL pristane (Sigma-Aldrich, USA). The mice were randomly assigned to two groups receiving daily i.p. injections of saline or liraglutide (2 mg/kg/day, Novo Nordisk, Denmark). The treatment was initiated either 14 days prior to DAH induction (preventive regimen) or on the day of pristane injection (early interventional regimen) and continued until 14 days post-modeling. Mice receiving the early interventional regimen were evaluated for gross pathology only. Mice under the preventive regimen were used for comprehensive analysis, including assessment of hemorrhage severity, lung inflammation, and immune cell infiltration.

All animal procedures were approved by the Animal Care and Use Committee of the Laboratory Animal Research Center of the Second Xiangya Hospital, Central South University.

2.2. ELISA

The serum was collected upon the sacrifice of mice. The concentrations of anti-ANA (IgG), total IgG, and total IgM antibodies in mouse serum were quantified using ELISA quantification kits (CUSABIO, Wuhan, China) according to the manufacturer's instructions. To measure the serum levels of anti-dsDNA IgM antibodies, 96-well plates were coated overnight at 4 °C with calf thymus DNA (MedChemExpress, USA) at 3 μg/mL in carbonate buffer. After blocking with 5 % BSA for 1 h at room temperature, diluted mouse serum samples (1:100) were added and incubated for 1.5 h at room temperature. Bound IgM was detected using an HRP-conjugated goat anti-mouse IgM secondary antibody (SouthernBiotech, 1:3000), followed by TMB substrate (SinoBiological, Beijing, China) development. Absorbance was read at 450 nm using a FlexA-200 Microplate Reader (ALLSHENG, Hangzhou, China).

2.3. Lung pathological evaluation

Lung tissues were first graded based on gross pathological examination into four categories according to hemorrhage severity: severe, moderate, mild, and no bleeding. Histopathological evaluation was subsequently performed using hematoxylin and eosin (H&E) staining and Prussian blue staining. For H&E-stained sections, four randomly selected 20 × fields per mouse were examined and scored based on the percentage of alveolar area affected by hemorrhage: 0 (no hemorrhage), 1 (0–25 % hemorrhage), 2 (25–50 % hemorrhage), 3 (50–75 % hemorrhage), and 4 (75–100 % hemorrhage). To further assess hemorrhagic activity, Prussian blue histochemical staining was employed to detect and quantify hemosiderin-laden macrophages in lung tissues. All stained sections were scanned and analyzed using CaseViewer 2.4.0.

2.4. Flow cytometry analysis

Single-cell suspensions were prepared from freshly isolated mouse lung tissues. Specifically, tissues were enzymatically digested using a dissociation kit (Miltenyi Biotec, Germany) and mechanically dissociated using the gentleMACS™ Dissociator. Then, the cell suspension was filtered through a 70-μm strainer and subjected to density gradient centrifugation using Percoll™ (Cytiva, USA) for leukocyte enrichment. For immunophenotyping, cells were first blocked with an anti-mouse CD16/32 antibody (BD Biosciences, USA) and stained with antibodies against surface markers in PBS containing 5 % FBS for 30 min at 4 °C in the dark. For intracellular and intranuclear staining, cells were fixed and permeabilized with a Transcription Factor Buffer Set (BD Pharmingen™, USA) for 40 min, and then stained with fluorescent antibodies for an additional 60 min at 4 °C in the dark. All samples were acquired on a CYTEK NL-3000 (Cytek Biosciences, USA), and analyzed using Three Star FlowJo (10.8.1). Antibodies used in our study were summarized in.

2.5. Lung immunohistochemistry

Murine lung tissues were fixed in 4 % PFA, dehydrated through a graded ethanol series, and embedded in paraffin. Sections of 4 μm were placed on Superfrost Plus slides (Thermo Fisher Scientific, USA). After deparaffinization and antigen retrieval, sections were incubated for 1 h at room temperature with primary antibodies against B220, CD11b, CD4, CD68, and Ly6G (all from Abcam, UK). This was followed by incubation with a species-matched HRP-conjugated secondary antibody (Abcam, UK) at RT for 30 min and Opal fluorophores diluted 1:100–1:300 in tyramide signal amplification (TSA) reagent (PerkinElmer, Taiwan, China) for 20 min at RT. Sequential staining cycles were carried out with heat-mediated antigen retrieval between each round to enable multiple target labeling. Nuclei were visualized using 4′,6-diamidino-2-phenylindole (DAPI). Whole-slide imaging was performed using a PerkinElmer Vectra multispectral imaging system (PerkinElmer, Taiwan, China), and image analysis was conducted with inForm 2.3.1 software (PerkinElmer, Taiwan, China).

2.6. Western blot analysis

Total proteins of lung tissues were extracted with whole cell lysis buffer and centrifuged at 12000 g for 15 min at 4 °C. Subsequently, a BCA Protein Assay Kit (Beyotime Biotechnology, China) was used to determine the protein concentrations. Equal amounts of protein were suspended in 1 × loading buffer, denatured at 100 °C for 5 min. The cellular proteins were then separated using SDS polyacrylamide gel electrophoresis (PAGE) and transferred to polyvinylidene difluoride (PVDF) membranes. Subsequently, the membranes were blocked with blocking buffer (NCM Biotech, China) for 15 min and then incubated overnight at 4 °C with a rabbit anti-CD163 antibody (1:1000) (Abcam, UK), a rabbit anti-CD86 antibody (1:1000) (Abcam, UK), and a rabbit anti-GADPH antibody (1:5000) (Proteintech, China). After three 10-min washes with PBST, the membranes were incubated with species-appropriate HRP-conjugated secondary antibodies for 1 h at room temperature. Finally, membranes were incubated with Luminol reagent (Santa Cruz Biotechnology, USA) and exposed to X-ray films.

2.7. Statistical analysis

All data are presented as the mean ± SD. Normality and homogeneity of variances were verified prior to statistical analysis. For comparisons between two groups with normal distribution and equal variances, a two-tailed unpaired Student's t-test was used. Otherwise, the Mann–Whitney *U* test was applied for non-parametric data. For data involving two factors, Two-way ANOVA was employed. Frequency data were analyzed by Fisher's exact test. Statistical analyses were conducted using GraphPad Prism 9.5.0. A p-value of less than 0.05 was considered statistically significant.

3. Results

3.1. Liraglutide treatment had no significant impact on body weight and glucose levels in a murine model of lupus-associated DAH

We established a murine model of lupus-associated DAH with a consistent incidence rate of approximately 67 % by administering a single intraperitoneal (i.p.) injection of 0.5 mL pristane (Fig. S1). To evaluate the therapeutic potential of liraglutide, mice were treated daily with i.p. injections of either saline or liraglutide, starting either on the day of pristane injection (early interventional regimen) or 14 days prior (preventive regimen) and continuing until 14 days post-modeling (Fig. S2A). Considering the glucoregulatory properties of liraglutide, body weight and random blood glucose levels were monitored throughout the experimental period. Liraglutide treatment induced a transient reduction in body weight during the first week of administration, after which body weight gradually recovered to levels comparable to the saline group. Following pristane injection, both groups exhibited a steady increase in body weight over time (Fig. S2B). In contrast, random blood glucose measurements revealed no significant differences between the liraglutide and saline groups at any time point (Fig. S2C).

3.2. Liraglutide reduced the incidence and ameliorated the severity of DAH in pristane-induced lupus mice

Gross pathological assessment demonstrated that liraglutide treatment significantly reduced the extent of pulmonary hemorrhage. In the early interventional regimen, 5 mice in saline group exhibited severe DAH (5/10) and the remaining 5 displayed mild DAH. By contrast, in the liraglutide group, severe, moderate, and mild DAH were observed in 2, 1, and 2 mice, respectively, with the other 5 showing no hemorrhage (Fig. S2D and S2E). Under the preventive regimen, 5 mice exhibited severe DAH (5/10) and 1 displayed mild DAH (1/10) in the saline group, whereas liraglutide group conversely exhibited only a single case of mild DAH (1/10) and no hemorrhage in the remaining 9 mice (Fig. 1A and B). Consistent with this protective effect, liraglutide administration significantly decreased lung wet weight compared to saline controls (Fig. 1C). Concomitant with the attenuation of DAH, liraglutide treatment led to a significant reduction in serum total IgG levels and anti-dsDNA IgM levels (Fig. 1D), which likely signifies a broad suppression of humoral immune responses by liraglutide. Histopathological evaluation of H&E-stained sections further confirmed these findings, with the liraglutide group displaying a markedly lower DAH score than the saline group (Fig. 2A and B). Prussian blue staining, which was applied to identify hemosiderin-laden macrophages resulting from erythrocyte phagocytosis, revealed minimal hemosiderin deposition in liraglutide-treated lungs, in sharp contrast to the extensive deposition observed in saline-treated controls (Fig. 2C and D).

3.3. Liraglutide reduced the infiltration of T cell and B cell subsets in the lungs

Previous studies have demonstrated a lower incidence of DAH in B6 Rag1$^{-/-}$ mice compared with wild-type B6 mice, suggesting that B and/or T cells may contribute to the development of DAH [10]. To investigate whether the protective effect of liraglutide involves modulation of pulmonary T and B cell infiltration, we performed flow cytometric analysis of digested lung tissues (Fig. S3). viSNE (t-distributed stochastic neighbor embedding–based visualization) of live CD45$^+$ cells from the lungs of saline- and liraglutide-treated mice revealed distinct immune cell distribution patterns (Fig. 3A). Quantitative analysis showed significant reductions in B220$^+$ cells, naïve B cells, CD19$^+$CD44$^+$ cells, CD19$^+$CD62L$^+$ cells, CD3$^+$CD4$^+$ T cells, CD3$^+$CD8$^+$ T cells, CD4$^+$ effector memory T (TEM) cells, and CD8$^+$ TEM cells in liraglutide-treated mice (Fig. 3B). Cell clusters in the viSNE map were annotated based on the expression of lineage-specific markers (Fig. 3C). In parallel, immunohistochemistry staining of lung sections for B220, CD4, and CD11b confirmed that liraglutide treatment significantly reduced the proportions of B220$^+$ and CD4$^+$ cells (Fig. 3D and E), corroborating the flow cytometry findings.

3.4. Liraglutide enhanced the population of alveolar macrophages in the lung

Myeloid cells, particularly neutrophils and macrophages, are the key effector cells in the pathogenesis of lupus-associated DAH and correlate strongly with its clinical severity. To determine whether liraglutide influences myeloid cell composition in the lung, we performed flow cytometric and viSNE analysis on CD45$^+$ cells from digested lung tissues of saline- and liraglutide-treated mice (Figure S4 and Fig. 4A). Liraglutide treatment substantially reshaped the pulmonary myeloid landscape

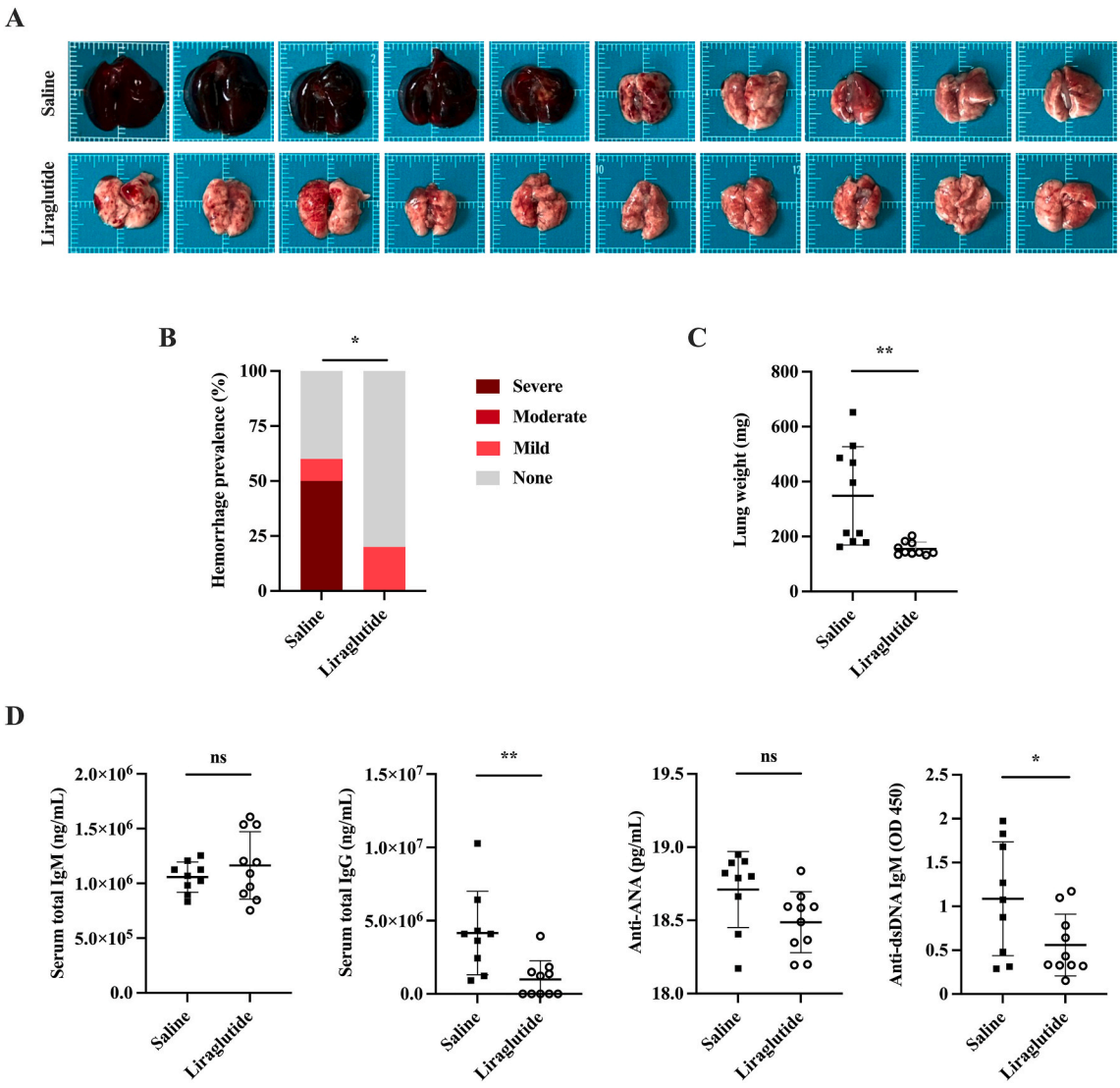

Fig. 1. Liraglutide reduced the incidence of DAH in pristane-induced lupus mice. (A) Gross images of lungs from the two groups (n = 10). (B) The incidence of DAH assessed by gross pathology. DAH severity was categorized into four grades: severe, moderate, mild, and none. (C) Quantification of fresh lung weight (n = 10). (D) Serum levels of total IgM, total IgG, anti-ANA, and anti-dsDNA IgM autoantiboides were measured by ELISA (n = 10). Data were shown as mean ± SD. Unpaired student's *t*-test for (A and D) and Fisher's exact test for (C). $*P < 0.05$, $**P < 0.01$, ns: not significant.

(Fig. 4A). Specifically, liraglutide-treated mice exhibited a significant increase in alveolar macrophages (AMs, $CD11c^{+}Siglec\text{-}F^{+}$) and dendritic cells ($CD11b^{+}CD24^{+}$) compared to saline-treated controls (Fig. 4B). Myeloid cell subsets within the viSNE landscape were annotated according to established lineage markers (Fig. 4C).

3.5. *Liraglutide promoted M2 polarization of pulmonary macrophages*

Previous studies in murine lupus models indicates that promoting M2 macrophage polarization can attenuate lupus-associated DAH [32]. Given this context, we further investigated whether liraglutide modulates pulmonary macrophage polarization. Flow cytometric analysis revealed that liraglutide treatment had no effects on M1 macrophages but significantly increased the abundance of anti-inflammatory M2 macrophages ($CD206^{+}$) within both interstitial macrophages (IMs, $CD11b^{+}CD64^{+}$) and AMs ($CD11c^{+}Siglec\text{-}F^{+}$) in the lung (Figure S4, Fig. 5A and B), accompanied by significantly elevated CD206 mean fluorescence intensity compared to saline controls (Fig. 5C). Western blot analysis was performed to assess the protein levels of the M2 marker CD163 and the M1 marker CD86 in lung tissues (Fig. 5D). Consistent with the flow cytometry data, liraglutide treatment significantly upregulated CD163 expression. In contrast, CD86 expression showed a decreasing trend but did not reach statistical significance (Fig. 5D). Collectively, these results demonstrated that liraglutide promoted a shift toward an M2-like anti-inflammatory phenotype in pulmonary macrophages.

4. Discussion

DAH represents one of the most devastating and life-threatening pulmonary complications in SLE patients [3]. It is pathologically characterized by alveolar and perivascular inflammation, hemorrhage, endothelial damage, and infiltration of macrophages, neutrophils, and lymphocytes [4]. The pathogenesis of SLE-associated DAH is complex and not fully elucidated, which contributes to the absence of standardized and target therapies. In this study, we established a pristane-induced murine model of lupus-associated DAH, and provided the first experimental evidence that liraglutide, a widely used GLP-1 receptor agonist, confers significant protection against lupus-associated DAH through multifaceted immunomodulatory

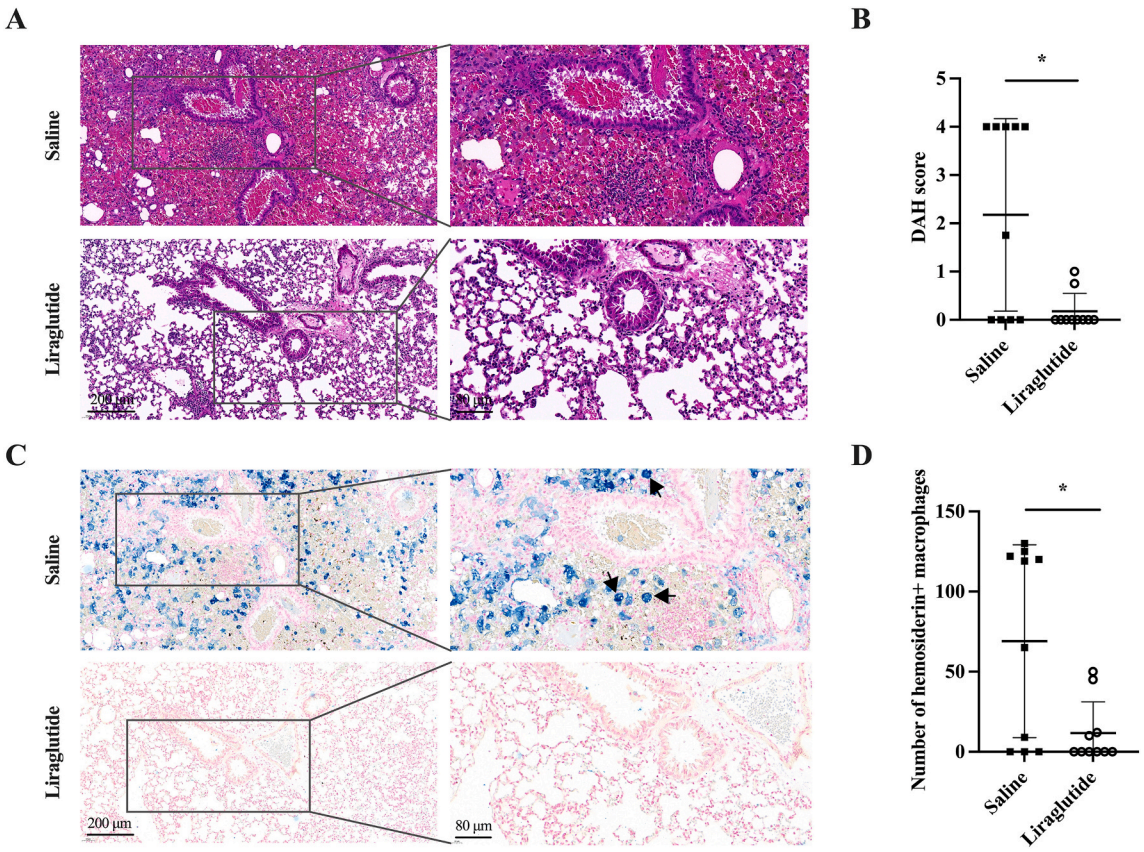

Fig. 2. Liraglutide attenuated the severity of pristane-induced DAH. (A) Representative images of H&E staining of lung tissue from mice treated with saline or liraglutide. Scale bar: left, 200 μm; right, 80 μm. (B) Statistical analysis of histopathological DAH scores in two groups based on H&E staining (n = 10). (C) Prussian blue staining of lung tissue from mice treated with saline or liraglutide. Black arrows indicate hemosiderin-laden macrophages. Scale bar: left, 200 μm; right, 80 μm. (D) Quantification of hemosiderin-laden macrophages in the lungs (n = 10). Data were shown as mean ± SD. Mann–Whitney *U* test for (B) and unpaired student's *t*-test for (D). *$P < 0.05$.

mechanisms.

The pristane-induced lupus model is particularly valuable for studying lupus-associated DAH. A single intraperitoneal injection of this saturated hydrocarbon oil triggers a well-established lupus-like autoimmune syndrome, including the production of characteristic autoantibodies and the development of immune-complex mediated tissue injury over time [33]. Notably, pristane migrates to the lung tissue shortly after administration, inducing a pathological process within 1–2 weeks that closely resembles human SLE-associated pulmonary hemorrhage, characterized by alveolar capillaritis, endothelial injury, and hemorrhage accompanied by a substantial inflammatory infiltrate [34]. However, unlike human SLE-associated DAH, this model does not show prominent immune complex deposition in the lungs [34,35]. This difference likely reflects distinct initiating mechanisms—pristane elicits a direct hydrocarbon-induced cellular injury, whereas human DAH often arises in the context of chronic autoimmunity and immune complex accumulation. Despite this difference in triggering events, downstream inflammatory and cellular pathways appear to be shared. Studies have demonstrated that pristane-induced model still requires IgM and complement (C3) for DAH development. This indicates that opsonization of injured/dead cells by natural IgM and complement activation still plays a crucial role, possibly via engagement of complement receptors (e.g., CR3/CR4) on macrophages. Moreover, macrophage depletion abolishes DAH in this model, underscoring the centrality of macrophage-driven inflammation [34]. Similarly, B cell depletion significantly reduces its incidence, demonstrating the important contributing role of the humoral immune response [10]. Thus, it remains a valuable tool for dissecting the shared inflammatory and cellular phases of alveolar injury, which are likely common across different etiologies of DAH. Among various murine lupus models, the pristane-induced model is unique in its consistent recapitulation of DAH, making it a highly relevant tool for our investigation.

Dysregulated T and B lymphocytes play central roles in the pathogenesis of SLE, wherein autoreactive B cells generate pathogenic autoantibodies that form immune complexes, activate complement, and recruit inflammatory cells, while T cells facilitate B cell activation and amplify tissue inflammation through cytokine secretion [36]. A similar involvement of B and T cells has been implicated in the development of DAH [8]. The critical role of B cells in DAH pathogenesis is highlighted by studies showing that B cell–deficient mice (e.g., B6 $Rag^{-/-}$ and B6 $Ig\mu^{-/-}$) exhibit a lower incidence of pristane-induced DAH, and that reconstitution of B cells restores susceptibility to DAH. In contrast, T cell receptor–deficient mice show no significant difference in DAH incidence compared with wild-type controls, suggesting a more supportive role for T cells in this complication [10]. In our study, liraglutide significantly reduced pulmonary infiltration of both T and B cells, indicating that modulation of adaptive immunity may contribute to its protective effects against DAH. However, the precise molecular mechanisms remain to be fully elucidated. Given that GLP-1R is expressed on B and T cells, and GLP-1Rs depletion promotes lymphocyte proliferation, liraglutide may directly activate GLP-1Rs on B and T cells, thereby inhibiting their proliferation and infiltration in lungs [16]. Previous research has shown that GLP-1 inhibits chemokine-induced migration of human $CD4^+$ T cells by suppressing PI3K activity [37]. Moreover, GLP-1R agonists can inhibit the production of chemokines such as CXCL10 and CCL5 from endothelial and immune cells across multiple inflammatory conditions [38,39]. Therefore, liraglutide may suppress the expression of key chemokines by various pulmonary cells, including endothelial cells,

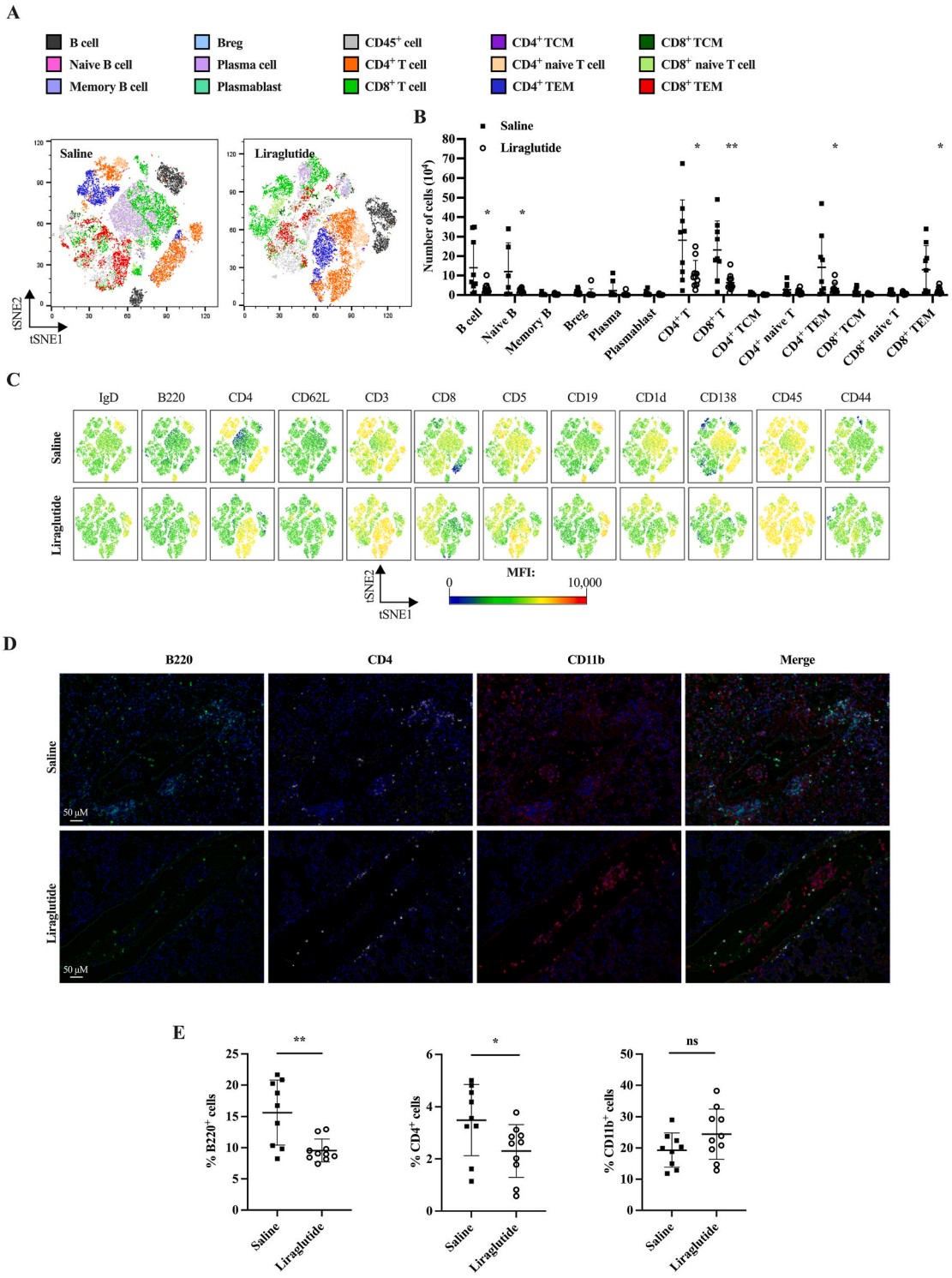

Fig. 3. Liraglutide inhibited the infiltration of T and B cells in the lungs. (A) viSNE visualization of pulmonary leukocytes from saline- and liraglutide-treated mice, analyzed by flow cytometry. (B) Statistical analysis of B cell ($CD45^+B220^+$), Naive B cell ($CD45^+B220^+CD138^-IgD^+$), Memory B cell ($CD45^+B220^+CD138^-IgD^-$), Reglulatory B cell (Breg, $CD45^+CD19^+CD1d^+CD5^+$), Plasma cell ($CD45^+CD19^-B220^{low/-}CD138^+$), Plasmablast ($CD45^+CD19^+B220^{low/-}CD138^+$), $CD4^+$ T cell ($CD3^+CD4^+$), $CD8^+$ T cell ($CD3^+CD8^+$), $CD4^+$ central memory T cell ($CD4^+$ TCM, $CD4^+CD62L^+CD44^+$), $CD4^+$ naive T cell ($CD4^+CD62L^+CD44^-$), $CD4^+$ effector memory T cell ($CD4^+$ TEM, $CD4^+CD62L^-CD44^+$), $CD8^+$ central memory T cell ($CD8^+$ TCM, $CD8^+CD62L^+CD44^+$), $CD8^+$ naive T cell ($CD8^+CD62L^+CD44^-$), and $CD8^+$ effector memory T cell ($CD8^+$ TEM, $CD8^+CD62L^-CD44^+$) (n = 10). (C) Expression patterns of key lineage markers. (D, E) Representative immunofluorescence images (D) and quantification (E) of $B220^+$ (green), $CD4^+$ (silver), and $CD11b^+$ (red) cells in lung sections. Nuclei were counterstained with DAPI (blue). Scale bars: 50 μm. Data were shown as mean ± SD. Unpaired student's *t*-test. $^*P < 0.05$, $^{**}P < 0.01$, ns: not significant.

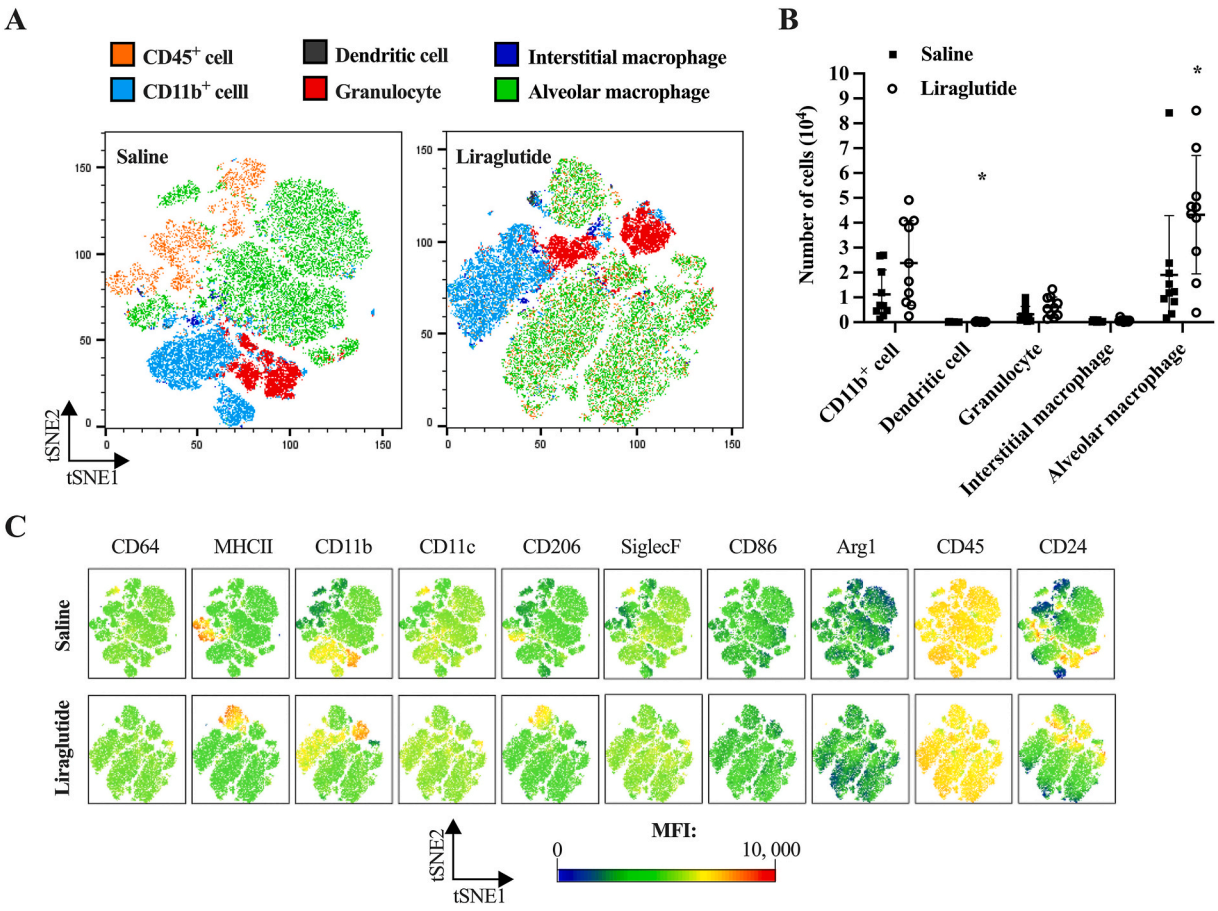

Fig. 4. Liraglutide increased alveolar macrophages in the lungs. (A, B) viSNE display (A) and quantitative analysis (B) of infiltrating myeloid cell subpopulations in the lungs of saline- and liraglutide-treated mice (n = 10). The cell subsets are defined as follows: $CD11b^+$ cell ($CD45^+CD11b^+$), dendritic cell (DC, $CD45^+CD11b^+MHCII^+CD24^+$), granulocyte ($CD45^+CD11b^+MHCII^-CD24^+$), interstitial macrophages (IM, $CD45^+CD11b^+MHCII^+CD64^+CD24^-$), and alveolar macrophage (AM, $CD45^+CD11b^{low/-}CD11c^+SiglecF^+$). (C) Expression patterns of key myeloid markers projected onto the t-SNE plot in (A). Data were presented as mean ± SD. Unpaired student's *t*-test. $^*P < 0.05$, $^{**}P < 0.01$.

alveolar epithelial cells, and resident immune cells, thereby disrupting the chemotactic signals required for T and B cell recruitment. Concurrently, liraglutide exerts a potent stabilizing effect on the vascular endothelium. By activating the GLP-1R, it enhances endothelial nitric oxide (NO) production and reduce the expression of adhesion molecules such as VCAM-1 and ICAM-1. These effects collectively stabilize the endothelial barrier, decrease vascular permeability, and inhibit leukocyte adhesion and transendothelial migration [23,40–42]. Thus, liraglutide may also attenuate T and B cell infiltration by suppressing adhesion molecule expression on pulmonary vascular endothelial cells and enhancing endothelial barrier integrity.

Beyond its effects on adaptive immunity, liraglutide profoundly influenced the pulmonary macrophage compartment. Macrophages in the lung are heterogeneous, with distinct subsets and functional states playing different, sometimes opposing, roles in injury and repair. Lung-resident macrophages include AMs and IMs, where AMs constitute the first line of defense in the alveoli and airways, whereas IMs act as gatekeepers of the lung interstitium and vasculature. Furthermore, macrophages can polarize into distinct functional phenotypes in response to microenvironmental signals. The classically activated M1 phenotype, typically induced by IFN-γ and LPS, promotes tissue injury and inflammation via expressing pro-inflammatory cytokines like TNF-α, IL-1β, and IL-6, while the alternatively activated M2 phenotype, polarized by IL-4 or IL-13, upregulates anti-inflammatory mediators like IL-10 and TGF-β to facilitate tissue repair and inflammation resolution [43,44]. A critical finding in pristane-induced DAH is the early depletion of resident $CD11c^+Siglec\text{-}F^+$ AMs, a phenomenon aligned with the 'macrophage disappearance reaction' observed during acute lung inflammation which may be attributed to cell death, loss of survival signals due to epithelial injury, or detachment followed by mucociliary clearance [43,45]. The loss of homeostatic, pro-repair AMs likely creates a permissive environment for unchecked inflammation and vascular damage [46]. Concurrently, there is an influx of monocyte-derived macrophages which, in the inflammatory milieu, often adopt an M1 phenotype, secreting cytokines that exacerbate tissue injury [45].

Our data demonstrate that liraglutide orchestrates a dual modulation of this macrophage response, which may be central to its protective effect. First, liraglutide reversed the pristane-induced loss of $CD11c^+Siglec\text{-}F^+$ AMs, indicating that liraglutide may promote the preservation, local proliferation, or timely repopulation of this crucial homeostatic niche, thereby restoring a first line of defense and repair capacity in the alveoli. Second, liraglutide drove a functional shift of the lung macrophages towards an anti-inflammatory, pro-resolving phenotype, as evidenced by increased expression of canonical M2 markers (CD163 and CD206) associated with tissue repair, efferocytosis, and the production of anti-inflammatory mediators [47]. Therefore, liraglutide exerts a coordinated two-pronged therapeutic strategy. It preserves the protective resident AMs while simultaneously biasing the infiltrating and local macrophages towards a healing M2 state. This dual effect would synergistically dampen the immune-driven lung injury, enhance the clearance of hemorrhage-derived debris, and promote tissue repair, ultimately preventing the development of severe DAH. The finding that liraglutide promotes M2 polarization aligns with prior evidence from other disease models. Specifically, in disease models such as hepatic

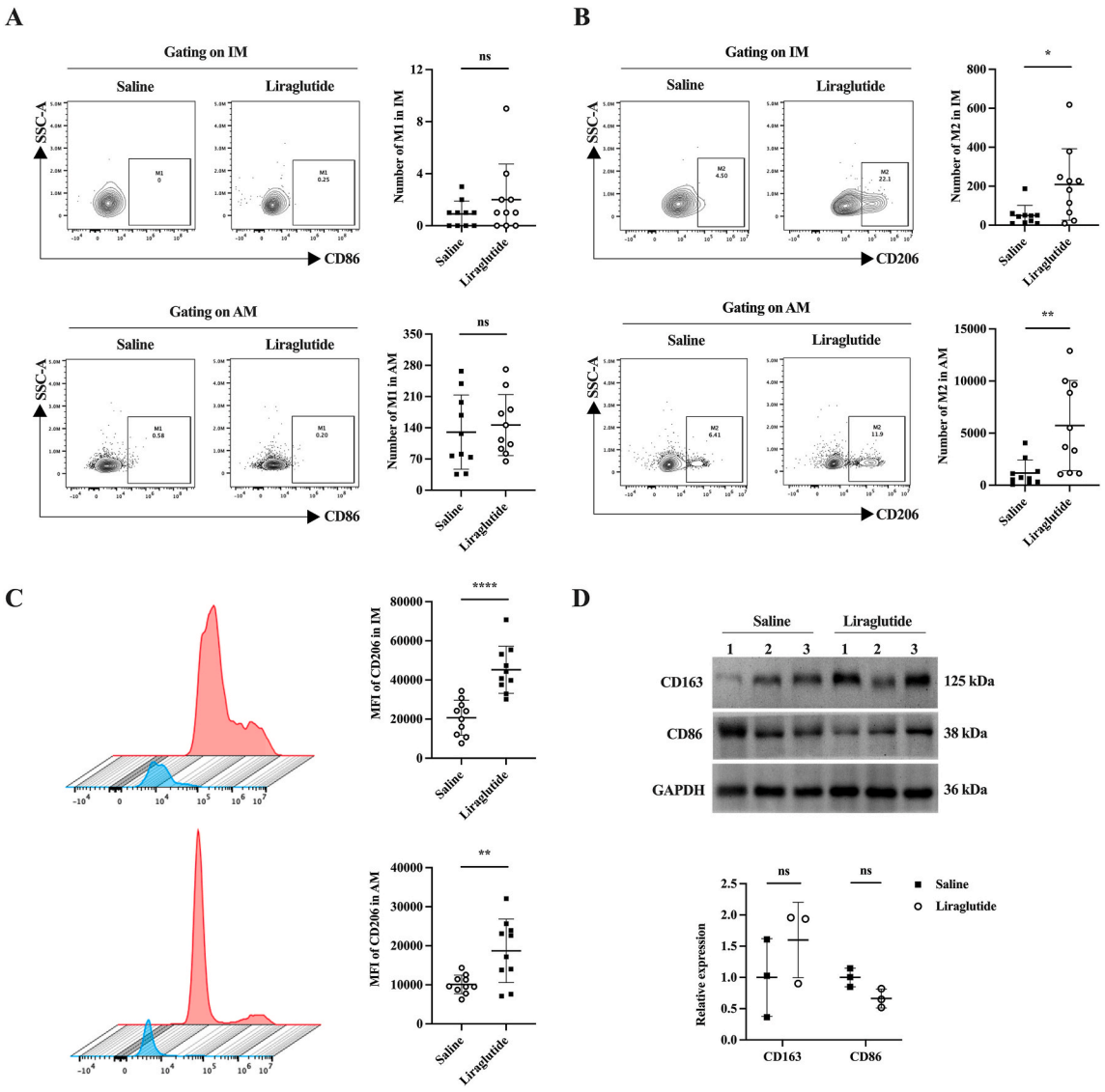

Fig. 5. Liraglutide promoted M2 macrophage polarization. (A, B) Flow cytometric analysis of the frequency of M1 (A) and M2 (B) macrophages in lung interstitial macrophages (IMs) and alveolar macrophages (AMs) (n = 10). (C) Mean fluorescence intensity (MFI) of CD206 in IMs and AMs (n = 10). (D) Representative western blots (up) and quantitative analysis (down) of CD163 and CD86 expression in lung tissues of the two groups (n = 3). Data is shown as mean ± SD. Unpaired student's *t*-test. $^{*}P < 0.05$, $^{**}P < 0.01$, $^{****}P < 0.0001$, ns: not significant.

ischemia-reperfusion injury and aortic aneurysm/dissection, liraglutide has been shown to exert protective effects by suppressing M1 macrophage polarization via GLP-1R [48,49]. Pretreatment with GLP-1R agonists in human monocyte-derived macrophages and murine Raw264.7 cells suppresses LPS-induced pro-inflammatory cytokines and promotes an M2-like phenotype characterized by STAT3 activation and increased IL-10 secretion [50,51]. Given that M2 polarization often involves activation of STAT3 and CREB [51], future studies should focus on validating the involvement of these pathways.

In summary, this study provides the first evidence that liraglutide treatment exerts a protective effect in a pristane-induced murine model of lupus-associated DAH. The prophylactic and therapeutic benefit is associated with reduced pulmonary recruitment of T and B cells and promotion of M2 macrophage polarization. These findings not only propose a novel prevent and treatment strategy for SLE-associated DAH but also expand the potential applications of GLP-1RAs in autoimmune diseases. However, several limitations of our study should be acknowledged. The specific mechanisms by which liraglutide reduces T and B cell infiltration, while proposed, require further direct validation through in vitro migration and adhesion assays. Similarly, the signaling pathways involved in liraglutide-induced M2 polarization need further dissection. Lastly, translational validation in clinical cohorts is essential to assess the relevance of these findings in human SLE.

CRediT authorship contribution statement

Li Jiang: Writing – review & editing, Writing – original draft, Investigation. **Liting He:** Writing – review & editing, Writing – original draft, Investigation. **Duo Li:** Methodology. **Xin Luo:** Investigation. **Ming Yang:** Methodology. **Haijing Wu:** Methodology. **Hai Long:** Writing – review & editing, Supervision, Funding acquisition, Conceptualization.

Funding

This work was supported by the National Natural Science Foundation of China (No. 82273540), the Science and Technology Innovation Program of Hunan Province (No. 2023RC1031, No. 2023JJ10089, No. 2016SK4001), and the Talent Program of Changsha Bureau of Science and Technology (No. kq2206008).

Declaration of competing interest

The authors declare that they have no known competing financial interests or personal relationships that could have appeared to influence the work reported in this paper.

Appendix A. Supplementary data

Supplementary data to this article can be found online at https://doi.org/10.1016/j.jtauto.2026.100349.

Data availability

Data will be made available on request.

References

[1] L. Durcan, T. O'Dwyer, M. Petri, Management strategies and future directions for systemic lupus erythematosus in adults, Lancet 393 (2019) 2332–2343.
[2] M. Kiriakidou, C.L. Ching, Systemic Lupus erythematosus, Ann. Intern. Med. 172 (2020) Itc81–itc96.
[3] S. Di Bartolomeo, A. Alunno, F. Carubbi, Respiratory manifestations in systemic lupus erythematosus, Pharmaceuticals 14 (2021).
[4] M.D. Hughson, Z. He, J. Henegar, R. McMurray, Alveolar hemorrhage and renal microangiopathy in systemic lupus erythematosus, Arch. Pathol. Lab Med. 125 (2001) 475–483.
[5] M.F. Liu, J.H. Lee, T.H. Weng, Y.Y. Lee, Clinical experience of 13 cases with severe pulmonary hemorrhage in systemic lupus erythematosus with active nephritis, Scand. J. Rheumatol. 27 (1998) 291–295.
[6] C. Abud-Mendoza, E. Diaz-Jouanen, D. Alarcón-Segovia, Fatal pulmonary hemorrhage in systemic lupus erythematosus. Occurrence without hemoptysis, J. Rheumatol. 12 (1985) 558–561.
[7] N.K. Al-Adhoubi, J. Bystrom, Systemic lupus erythematosus and diffuse alveolar hemorrhage, etiology and novel treatment strategies, Lupus 29 (2020) 355–363.
[8] R. Huo, X. Huang, J. Lin, Systemic lupus erythematosus with diffuse alveolar hemorrhage, Chin Med J (Engl) 136 (2023) 2883–2885.
[9] P.A. Jarrot, E. Tellier, L. Plantureux, L. Crescence, S. Robert, C. Chareyre, et al., Neutrophil extracellular traps are associated with the pathogenesis of diffuse alveolar hemorrhage in murine lupus, J. Autoimmun. 100 (2019) 120–130.
[10] T.T. Barker, P.Y. Lee, K.M. Kelly-Scumpia, J.S. Weinstein, D.C. Nacionales, Y. Kumagai, et al., Pathogenic role of B cells in the development of diffuse alveolar hemorrhage induced by pristane, Lab. Invest. 91 (2011) 1540–1550.
[11] S. Han, H. Zhuang, S. Shumyak, J. Wu, H. Li, L.J. Yang, et al., A novel subset of anti-inflammatory CD138(+) macrophages is deficient in mice with experimental lupus, J. Immunol. 199 (2017) 1261–1274.
[12] W.V. Tamborlane, M. Barrientos-Pérez, U. Fainberg, H. Frimer-Larsen, M. Hafez, P. M. Hale, et al., Liraglutide in children and adolescents with type 2 diabetes, N. Engl. J. Med. 381 (2019) 637–646.
[13] L.J. Scott, Liraglutide: a review of its use in the management of obesity, Drugs 75 (2015) 899–910.
[14] G. Bendotti, L. Montefusco, M.E. Lunati, V. Usuelli, I. Pastore, E. Lazzaroni, et al., The anti-inflammatory and immunological properties of GLP-1 Receptor agonists, Pharmacol. Res. 182 (2022) 106320.
[15] C. Pyke, R.S. Heller, R.K. Kirk, C. Ørskov, S. Reedtz-Runge, P. Kaastrup, et al., GLP-1 receptor localization in monkey and human tissue: novel distribution revealed with extensively validated monoclonal antibody, Endocrinology 155 (2014) 1280–1290.
[16] I. Hadjiyanni, K.A. Siminovitch, J.S. Danska, D.J. Drucker, Glucagon-like peptide-1 receptor signalling selectively regulates murine lymphocyte proliferation and maintenance of peripheral regulatory T cells, Diabetologia 53 (2010) 730–740.
[17] J.P. Wei, C.L. Yang, W.H. Leng, L.L. Ding, G.H. Zhao, Use of GLP1RAs and occurrence of respiratory disorders: a meta-analysis of large randomized trials of GLP1RAs, Clin Respir J 15 (2021) 847–850.
[18] L. Zhang, L. Han, Y. Lu, Q. Chen, Liraglutide attenuates autoimmune myocarditis by inhibiting NLRP3 and NF-κb pathways, Sci. Rep. 15 (2025) 27274.
[19] R.A. Ammar, A.F. Mohamed, M.M. Kamal, M.M. Safar, N.F. Abdelkader, Neuroprotective effect of liraglutide in an experimental mouse model of multiple sclerosis: role of AMPK/SIRT1 signaling and NLRP3 inflammasome, Inflammopharmacology 30 (2022) 919–934.
[20] S.H. Alharbi, Anti-inflammatory role of glucagon-like peptide 1 receptor agonists and its clinical implications, Ther Adv Endocrinol Metab 15 (2024) 20420188231222367.
[21] C. Meurot, C. Martin, L. Sudre, J. Breton, C. Bougault, R. Rattenbach, et al., Liraglutide, a glucagon-like peptide 1 receptor agonist, exerts analgesic, anti-inflammatory and anti-degradative actions in osteoarthritis, Sci. Rep. 12 (2022) 1567.
[22] D. Chen, H. Liang, L. Huang, H. Zhou, Z. Wang, Liraglutide enhances the effect of checkpoint blockade in lung and liver cancers through the inhibition of neutrophil extracellular traps, FEBS Open Bio 14 (2024) 1365–1377.
[23] M. Punjabi, A. Kosareva, L. Xu, A. Ochoa-Espinosa, S. Decembrini, G. Hofmann, et al., Liraglutide lowers endothelial vascular cell adhesion Molecule-1 in murine atherosclerosis independent of glucose levels, JACC Basic Transl Sci 8 (2023) 189–200.
[24] Y. Ding, Y. Peng, H. Wu, Y. Huang, K. Sheng, C. Li, et al., The protective roles of liraglutide on Kawasaki disease via AMPK/mTOR/NF-κB pathway, Int. Immunopharmacol. 117 (2023) 110028.
[25] K.D. Bjørnholm, G.F. Skovsted, A. Mitgaard-Thomsen, G. Rakipovski, P. Tveden-Nyborg, J. Lykkesfeldt, et al., Liraglutide treatment improves endothelial function in the Ldlr-/- mouse model of atherosclerosis and affects genes involved in vascular remodelling and inflammation, Basic Clin. Pharmacol. Toxicol. 128 (2021) 103–114.
[26] J. Guo, X. Zhang, R. Pan, Y. Zheng, W. Chen, L. Wang, Liraglutide alleviates sepsis-induced acute lung injury by regulating pulmonary surfactant through inhibiting autophagy, Immunopharmacol. Immunotoxicol. 46 (2024) 573–582.
[27] B. Baer, N.D. Putz, K. Riedmann, S. Gonski, J. Lin, L.B. Ware, et al., Liraglutide pretreatment attenuates sepsis-induced acute lung injury, Am. J. Physiol. Lung Cell. Mol. Physiol. 325 (2023). L368-l84.
[28] F. Zhou, Y. Zhang, J. Chen, X. Hu, Y. Xu, Liraglutide attenuates lipopolysaccharide-induced acute lung injury in mice, Eur. J. Pharmacol. 791 (2016) 735–740.
[29] C. Liu, Q. Zhang, H. Zhou, L. Jin, C. Liu, M. Yang, et al., GLP-1R activation attenuates the progression of pulmonary fibrosis via disrupting NLRP3 inflammasome/PFKFB3-driven glycolysis interaction and histone lactylation, J. Transl. Med. 22 (2024) 954.
[30] Y. Zhang, T. Liu, H. Guo, J. Shi, J. Yang, S. Fu, et al., Ex vivo lung perfusion with GLP-1R agonist mitigates ischemia/reperfusion injury through pyroptosis modulation in lung transplantation- an experimental study, Int. J. Surg. 111 (2025) 3781–3797.
[31] N.E. Viby, M.S. Isidor, K.B. Buggeskov, S.S. Poulsen, J.B. Hansen, H. Kissow, Glucagon-like peptide-1 (GLP-1) reduces mortality and improves lung function in a model of experimental obstructive lung disease in female mice, Endocrinology 154 (2013) 4503–4511.
[32] Z. Yang, L. Yan, H. Cao, Y. Gu, P. Zhou, M. Shi, et al., Erythropoietin protects against Diffuse alveolar hemorrhage in mice by regulating macrophage polarization through the EPOR/JAK2/STAT3 axis, J. Immunol. 206 (2021) 1752–1764.
[33] H.B. Richards, M. Satoh, M. Shaw, C. Libert, V. Poli, W.H. Reeves, Interleukin 6 dependence of anti-DNA antibody production: evidence for two pathways of autoantibody formation in pristane-induced lupus, J. Exp. Med. 188 (1998) 985–990.
[34] H. Zhuang, S. Han, P.Y. Lee, R. Khaybullin, S. Shumyak, L. Lu, et al., Pathogenesis of Diffuse alveolar hemorrhage in Murine Lupus, Arthritis Rheumatol. 69 (2017) 1280–1293.
[35] V.R. Chowdhary, J.P. Grande, H.S. Luthra, C.S. David, Characterization of haemorrhagic pulmonary capillaritis: another manifestation of Pristane-induced lupus, Rheumatology 46 (2007) 1405–1410.
[36] H. Li, A. Boulougoura, Y. Endo, G.C. Tsokos, Abnormalities of T cells in systemic lupus erythematosus: new insights in pathogenesis and therapeutic strategies, J. Autoimmun. 132 (2022) 102870.
[37] N. Marx, M. Burgmaier, P. Heinz, M. Ostertag, A. Hausauer, H. Bach, et al., Glucagon-like peptide-1(1-37) inhibits chemokine-induced migration of human CD4-positive lymphocytes, Cell. Mol. Life Sci. 67 (2010) 3549–3555.
[38] A. Ullah, B. Shen, Immunomodulatory effects of anti-diabetic therapies: cytokine and chemokine modulation by metformin, sodium-glucose cotransporter 2 inhibitors, and glucagon-like peptide-1 receptor agonists (2013-2025), Eur. J. Med. Chem. 299 (2025) 118065.
[39] M. Zhao, B. Liao, C. Yun, X. Qi, Y. Pang, Liraglutide improves follicle development in polycystic ovary syndrome by inhibiting CXCL10 secretion, Reprod. Biol. Endocrinol. 22 (2024) 98.
[40] S. Steven, K. Jurk, M. Kopp, S. Kröller-Schön, Y. Mikhed, K. Schwierczek, et al., Glucagon-like peptide-1 receptor signalling reduces microvascular thrombosis, nitro-oxidative stress and platelet activation in endotoxaemic mice, Br. J. Pharmacol. 174 (2017) 1620–1632.
[41] H. Kushima, Y. Mori, M. Koshibu, M. Hiromura, K. Kohashi, M. Terasaki, et al., The role of endothelial nitric oxide in the anti-restenotic effects of liraglutide in a mouse model of restenosis, Cardiovasc. Diabetol. 16 (2017) 122.
[42] T. Gaspari, H. Liu, I. Welungoda, Y. Hu, R.E. Widdop, L.B. Knudsen, et al., A GLP-1 receptor agonist liraglutide inhibits endothelial cell dysfunction and vascular adhesion molecule expression in an ApoE-/- mouse model, Diab Vasc Dis Res 8 (2011) 117–124.
[43] H. Aegerter, B.N. Lambrecht, C.V. Jakubzick, Biology of lung macrophages in health and disease, Immunity 55 (2022) 1564–1580.
[44] T. Shi, L. Denney, H. An, L.P. Ho, Y. Zheng, Alveolar and lung interstitial macrophages: definitions, functions, and roles in lung fibrosis, J. Leukoc. Biol. 110 (2021) 107–114.
[45] P.Y. Lee, N. Nelson-Maney, Y. Huang, A. Levescot, Q. Wang, K. Wei, et al., High-dimensional analysis reveals a pathogenic role of inflammatory monocytes in experimental diffuse alveolar hemorrhage, JCI Insight 4 (2019).
[46] H. Miki, H. Pei, D.T. Gracias, J. Linden, M. Croft, Clearance of apoptotic cells by lung alveolar macrophages prevents development of house dust mite-induced asthmatic lung inflammation, J. Allergy Clin. Immunol. 147 (2021), 1087-92.e3.
[47] M. Luo, F. Zhao, H. Cheng, M. Su, Y. Wang, Macrophage polarization: an important role in inflammatory diseases, Front. Immunol. 15 (2024) 1352946.
[48] S.L. Li, Z.M. Wang, C. Xu, F.H. Che, X.F. Hu, R. Cao, et al., Liraglutide Attenuates hepatic ischemia-reperfusion injury by modulating macrophage polarization, Front. Immunol. 13 (2022) 869050.
[49] K. Zhang, R. Li, Y. Matniyaz, R. Yu, J. Pan, W. Liu, et al., Liraglutide attenuates angiotensin II-induced aortic dissection and aortic aneurysm via inhibiting M1

macrophage polarization in APOE (-/-) mice, Biochem. Pharmacol. 223 (2024) 116170.
[50] C. Lu, T. Xie, X. Guo, D. Wu, S. Li, X. Li, et al., Glucagon-like peptide-1 receptor agonist exendin-4 mitigates lipopolysaccharide-induced inflammatory responses in RAW264.7 macrophages, Int. Immunopharmacol. 77 (2019) 105969.
[51] D. Shiraishi, Y. Fujiwara, Y. Komohara, H. Mizuta, M. Takeya, Glucagon-like peptide-1 (GLP-1) induces M2 polarization of human macrophages via STAT3 activation, Biochem. Biophys. Res. Commun. 425 (2012) 304–308.